A SHORT REVIEW OF ABLATIVE-MATERIAL RESPONSE MODELS AND SIMULATION TOOLS

J. Lachaud[1], **T. E. Magin**[2], **I. Cozmuta**[3], **and N. N. Mansour**[4]

[1]*Univ. California Santa Cruz/UARC, 94035 Moffett Field, CA, USA*
[2]*von Karman Institute, B-1640 Rhode-Saint-Genèse, Belgium*
[3]*ERC/NASA ARC, 94035 Moffett Field, CA, USA*
[4]*NASA Ames Research Center, 94035 Moffett Field, CA, USA*

ABSTRACT

A review of the governing equations and boundary conditions used to model the response of ablative materials submitted to a high-enthalpy flow is proposed. The heritage of model-development efforts undertaken in the 1960s is extremely clear: the bases of the models used in the community are mathematically equivalent. Most of the material-response codes implement a single model in which the equation parameters may be modified to model different materials or conditions. The level of fidelity of the models implemented in design tools only slightly varies. Research and development codes are generally more advanced but often not as robust. The capabilities of each of these codes are summarized in a color-coded table along with research and development efforts currently in progress.

Key words: Ablative material; modeling; design tool.

NOMENCLATURE

Latin

$\mathcal{F}_i$	Diffusion flux of the i^{th} species, $kg \cdot m^{-2} \cdot s^{-1}$
$\dot{m}$	Mass flow rate, $kg \cdot m^{-2} \cdot s^{-1}$
A_i	Gaseous species i
A_j	Arrhenius law pre-exponential factor, SI
C_H	Stanton number for heat transfer
C_M	Stanton number for mass transfer
c_p	Specific heat, $J \cdot kg^{-1} \cdot K^{-1}$
e	Specific energy, $J \cdot kg^{-1}$
E_j	Arrhenius law activation energy, $J \cdot kg^{-1}$
F_j	Fraction of mass lost through pyrolysis reaction j
h	Specific enthalpy, $J \cdot kg^{-1}$
j	Diffusive flux, $mol \cdot m^{-2} \cdot s^{-1}$
K_i	Chemical equilibrium constant for reaction i
l	Thickness or length, m
m_j	Arrhenius law parameter
M_k	Molar mass of species k, $kg \cdot mol^{-1}$
N_g	Number of gaseous species
n_j	Arrhenius law parameter
N_p	Number of pyrolysis reactions
q	Heat flux, $J \cdot m^{-2} \cdot s^{-1}$
R	Perfect gas constant, $J \cdot kg^{-1} \cdot K^{-1}$
v	Convection velocity, $m \cdot s^{-1}$
y	Mass fraction
Fo	Forchheimer number
K	Permeability
p	Pressure, Pa

Greek

β	Klinkenberg coefficient, Pa
ϵ	Volume fraction
γ_{ji}	Stoichiometric coefficient, reaction j species i
μ	Viscosity, $Pa \cdot s^1$
ω	Reaction rate, $mol \cdot m^{-3} \cdot s^{-1}$
ω^s	Solid reaction rate, $mol \cdot m^{-3} \cdot s^{-1}$
Π	Pyrolysis gas production rate, $kg \cdot m^{-3} \cdot s^{-1}$
ρ	Density, $kg \cdot m^{-3}$
τ	Characteristic time, s
ξ_j	Advancement of pyrolysis reaction j

Subscripts

a	Ablative material (gas, fiber, and matrix)
c	Char
e	Boundary layer edge properties
f	Reinforcement (non-pyrolyzing phase)
g	Gas phase
m, PM	Polymer matrix
mv	Virgin polymer matrix
p	Pyrolysis
pg	Pyrolysis gas
s	Solid phase

Conventions

$\partial_{\mathbf{x}} \cdot ()$	Divergence
$\partial_t ()$	Time derivative
$\underline{\underline{\mathbf{T}}}$	Second order tensor
$\overline{\mathbf{u}}$	Vector

1. INTRODUCTION

During re-entry, a fraction of the heat is transferred to the thermal protection system (TPS) leading to a gradual temperature increase of the material (figure 1). With the temperature increase, the virgin material is successively transformed and removed by two phenomena. The first transformation phenomenon is called pyrolysis. During pyrolysis, the pyrolyzing phase of the material (often a polymer matrix) progressively carbonizes and loses mass producing pyrolysis gases. The pyrolysis gases are transported out of the material by diffusion and convection through the pore network. During this transfer, their chemical composition evolves as their temperature increases. The second transformation phenomenon is the ablation of the char that is composed of the residual carbonized matrix and of the non-pyrolyzing phase (often a carbon or silicon-carbide fibrous preform). Depending on reentry conditions, ablation may be due to heterogeneous chemical reactions (oxidation, nitridation), phase change (sublimation), and/or mechanical erosion (spallation). Material response models should predict accurately the ablation rate and the peak temperature of the bondline at the interface of the TPS and the substructure. The first open literature publication providing a very detailed and comprehensive analysis of ablative material response in high enthalpy environments is the Aerotherm report from 1968 describing their suite of design tools [16]. CMA and ACE, Aerotherm's in-depth material response and surface ablation codes respectively, are cited as a reference in most publications in the field. The models implemented in current design-capable tools are mostly replicas (or parallel developments) of the Aerotherm model with slight variations. Interestingly, the modifications to the Aerotherm model have mainly involved simplifications, with some of the Aerotherm capabilities currently no longer maintained in most of the major tools. Recent interest in manned-rated and challenging design missions (e.g. high mass, very high velocity, porous materials) has raised the need for high-fidelity models capable of providing optimized design and comprehensive uncertainty quantifications. All the capabilities of the Aerotherm's suite of tools and the rich academic work on pyrolysis and ablation are being revisited and progressively introduced (or re-introduced) both in research codes and in design tools. In a complementary effort, several academic, government, and industrial teams are working on the development, the implementation, and the validation of original physics-based models that will enable anchoring of CMA/ACE-based design tools, accurate uncertainty analysis, and maybe become the future base models for design-rated codes. This paper first presents the pyrolysis-ablation problem through the governing equations (mass, momentum, and energy conservation) and boundary conditions. Different levels of modeling fidelity are presented and discussed. An effort was made to gather information on the simulation tools that are actively used either for design or for research and development. The capabilities of each of these codes are summed up in figure 4.

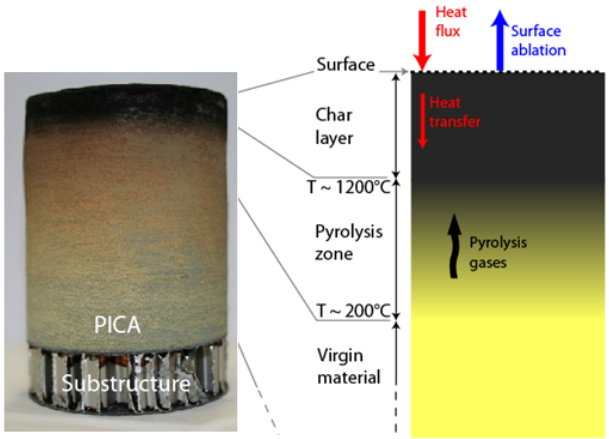

Figure 1. Picture of a core of ablative material extracted from the TPS of Stardust [33] and schematic of the zones of degradation illustrating the material response to a high-enthalpy flow.

2. CONSTITUTIVE MODELS

2.1. Mass conservation

The gaseous mass-conservation equation includes a production term (right-hand side) to account for the pyrolysis gas production, noted Π, and reads

$$\partial_t(\epsilon_g \rho_g) + \partial_{\mathbf{x}} \cdot (\epsilon_g \rho_g \mathbf{v_g}) = \Pi \qquad (1)$$

In several codes, the time derivative is omitted and the gas flow problem is treated as a succession of steady state problems (see section 4). This simplification is correct when the variation of the intensive variables (temperature, pressure) are slow compared to the characteristic time of the flow in the porous medium. The characteristic time of the pyrolysis gas flow, τ_{pg} may be defined as the ratio of the thickness of the char layer - l_c - to the velocity of the gas. In typical re-entry applications, $\tau_p g = l_c / v_g \simeq 0.01/1 = 0.01s$. Therefore, the omission of the time derivative is an acceptable practice for situations for which the variations of the intensive variables are negligible over time steps of $\tau_{pg} \ll \tau_{step} = 1s$. The determination of the direction of the gas velocity, $\mathbf{v_g}$, is necessary to solve the average mass-conservation equation. In several one-dimensional codes, this equation is numerically integrated with the assumption that the gas flow is perpendicular to the surface and directed towards the surface. This is exact in one-dimensional steady-state problems with an impermeable back face. In other conditions and in multi-dimensional problems, the direction of the flow has to be determined by resolution of the momentum-conservation equation.

The pyrolysis gas production is obtained by fitting thermogravimetry analysis of the resin decomposition using

one or several Arrhenius laws. For example, for phenolic polymers, it has been shown that the pyrolysis degradation process follows four steps [36], that may be described by four heterogeneous decomposition reactions [37]. A convenient notation for $j \in [1, N_p]$ pyrolysis reactions is

$$PM_j \rightarrow \sum_{i=1}^{N_g} \gamma_{ji} A_i \tag{2}$$

where PM_j is a fictive solid species of the pyrolysing polymer matrix (PM). The pyrolysing matrix density is then given by

$$\epsilon_m \rho_m = \epsilon_{mv} \rho_{mv} \sum_{j=1}^{N_p} F_j (1 - \xi_j) \tag{3}$$

where

$$\frac{\partial_t \xi_j}{(1-\xi_j)^{m_j}} = T^{n_j} \mathcal{A}_j \exp\left(-\frac{\mathcal{E}_j}{\mathcal{R}T}\right) \tag{4}$$

The pyrolysis-gas production is given by

$$\Pi = -\partial_t(\epsilon_m \rho_m) = \epsilon_{mv} \rho_{mv} \sum_{j=1}^{N_p} F_j \partial_t(\xi_j) \tag{5}$$

In the literature, the equations used to describe pyrolysis models vary but they are mathematically equivalent.

It is important to mention that state-of-the-art design codes do not track the species production. Only the average mass production -Π - is computed from the Arrhenius laws. A constant elemental fraction of the pyrolysis gas is assumed. The gas chemical composition and derived quantities (gas enthalpy, viscosity, mean molar mass) are then computed using the chemical equilibrium assumption or heuristic methods.

The pyrolysis gas production rate for each species i could readily be obtained using

$$\langle \pi_i \rangle^g = \epsilon_m \rho_{mv} \sum_{j=1}^{N_p} [\partial_t \xi_j \, F_j \, \widetilde{\gamma}_{ji}] \tag{6}$$

where

$$\widetilde{\gamma}_{ji} = \frac{\gamma_{ji}}{\sum_{k=1}^{N_g} \gamma_{jk} \mathcal{M}_k} \tag{7}$$

This requires the experimental determination of the stoechiometric factors - γ_{ji}, which are not directly available in the literature but may be derived from experimental studies [34, 36, 37]. The overall pyrolysis gas production may still by obtained from: $\Pi = \sum_{i=1}^{N_s} [\pi_i M_i]$.

Higher fidelity models are being developed and implemented. They account for species production, transport, and chemical reactions (finite-rate chemistry) within porous media. The species conservation equation may be written in mass fraction - y_i as

$$\partial_t(\epsilon_g \rho_g y_i) + \partial_{\mathbf{x}} \cdot (\epsilon_g \rho_g y_i \mathbf{v_g}) + \partial_{\mathbf{x}} \cdot \mathcal{F}_i = \pi M_i + \epsilon_g \omega_i M_i \tag{8}$$

Both pyrolysis species production - π_i - and chemical species production - ω_i - are needed. For the computation of ω_i, the finite-rate chemistry model developed by Pike and April in the late 1960s [28, 2] is used for preliminary analyses. This model was developed using chemical data and experimental techniques available at this time. Efforts are being undertaken in several teams to develop up-to-date finite-rate chemistry models and modern experimental set-ups for their validation [20]. $\mathcal{F}_i$ is the diffusion flux of the i^{th} species. At low pressures, mass transfer (diffusion) in porous media is not negligible compared to advection [18]. Mass transfer in porous media is a complex problem. The effective diffusion coefficient is smaller than the bulk diffusion coefficient due to the porosity and the tortuosity of the material [18]. Several models are available. A popular extension of the Stefan-Maxwell model [12] to porous media is the *dusty gas model* [25]. To our knowledge no fully capable ablation material-response code has such a capability yet. High-fidelity models including in-depth finite-rate chemistry will need to account for diffusion.

The solid-phase mass conservation is also integrated to compute the effective density of the solid. The volume-averaged density change of the matrix (due to pyrolysis -Π) is currently modeled using forms equivalent to

$$\partial_t(\epsilon_m \rho_m) = \Pi \tag{9}$$

which is easily derived from equation 5. The current assumption is that there is no ablation or coking in-depth. Coking is neglected and ablation is modeled as a surface phenomenon only. Therefore, ablation is accounted for using a prescribed recession velocity at the wall, handled as a boundary condition (rather than as an in-depth constitutive equation) as described in section 3.

Current research efforts aim at developing models for in-depth coking and ablation. For this application, the solid mass-conservation equation may be generalized to account for heterogeneous reactions

$$\partial_t(\epsilon_s \rho_s) = \partial_t(\epsilon_m \rho_m + \epsilon_f \rho_f) = -\Pi - \sum_{i \in s} \epsilon_g \omega_i^s M_i \tag{10}$$

However, the determination of the heterogeneous reaction rates -ω_i^s- is not an easy task and is still being investigated.

2.2. Momentum conservation in porous media

The average gas velocity is obtained by resolution of the momentum-conservation equation. In porous media, the volume-averaged momentum conservation may be written as

$$\mathbf{v_g} = -\frac{1}{\epsilon_g \mu} \frac{1+\beta/p}{1+Fo} \underline{\underline{\mathbf{K}}} \cdot \partial_t p \tag{11}$$

Most of the materials are anisotropic, therefore, the permeability - $\underline{\underline{\mathbf{K}}}$ - is a second order tensor. For example, Fiberform, the carbon preform of PICA [35], has orthotropic permeability properties [23]. For creeping (Stokes) flows in the continuum regime (in the pores of the material), the volume-average momentum conservation degenerates into Darcy's law ($\beta = 0$, $Fo = 0$). The term $1+\beta/p$ is the Klinkenberg correction to account for slip effects (at the pore scale) when the Knudsen number (ratio of the mean free path to the mean pore diameter) is not small. The term $1+Fo$ is the Forchheimer correction to account for high velocity effects at the pore scale (flow separation in the continuum regime). Typically, Forchheimer effects are expected to occur for pyrolysis gas velocities higher than $50\,m/s$ (that is, in high-density ablative materials submitted to very high heat fluxes). It is not advised to use both corrections simultaneously as they address different regimes.

2.3. Energy conservation

According to Puiroux [29], solid and gas phases are in thermal equilibrium as long as the Péclet number for diffusion of heat within the pores is small ($Pe = \epsilon_g \rho_g c_{p,g} d_p v_g / k_g$). In most of the applications of interest for space agencies, the small pore size ($< 100\mu m$) and the slow pyrolysis gas flow ($v_g \sim 1m/s$) insure a small Péclet number: the gas temperature accommodates to the solid temperature within the pores. Under the thermal equilibrium assumption, the energy conservation may be written as

$$\begin{aligned} \partial_t \rho_a e_a + \partial_{\mathbf{x}} \cdot (\epsilon_g \rho_g h_g \mathbf{v_g}) + \partial_{\mathbf{x}} \cdot \sum_{i=1}^{N_g} (h_i \mathcal{F}_i) \\ = \partial_{\mathbf{x}} \cdot (\underline{\underline{\mathbf{k}}} \cdot \partial_{\mathbf{x}} T) + \mu \epsilon_g^2 (\underline{\underline{\mathbf{K}}}^{-1} \cdot \mathbf{v}) \cdot \mathbf{v} \end{aligned} \tag{12}$$

where the total (storage) energy of the ablative material is the sum of the energy of its components

$$\rho_a e_a = \epsilon_g \rho_g e_g + \epsilon_m \rho_m h_m + \epsilon_f \rho_f h_f \tag{13}$$

The second and third terms of the left-hand side are the energy convected (advection) and the energy transferred (diffusion) by the pyrolysis gases, respectively. Heat transfer is conveniently modeled as an effective diffusive transfer (Fourier's law). The effective conductivity - $\underline{\underline{\mathbf{k}}}$ - is a second order tensor accounting for conduction in the solid, conduction in the gas, and effective radiative heat transfer. The validity of this volume-averaged approach is questionable. The main issue is the validity of the linearization of the radiative heat transfer. A theoretical study has shown that radiative heat transfer may be linearized for two-dimensional carbon-fiber preforms [40, 41]. The applicability to other materials is not straightforward and needs to be investigated. The second term on the right-hand side is the energy dissipated by viscous effects in Darcian regime [10]. It is small compared to the heat transfer term and often neglected.

3. BOUNDARY CONDITIONS

At the bondline, conservative boundary conditions are generally used (adiabatic and impermeable). At the wall and in ablative conditions, surface energy balance and surface mass balance are used as boundary conditions. [Of course, simple wall boundary conditions may always be used for simple analyses, e.g. fixed temperature.]

3.1. Surface energy balance

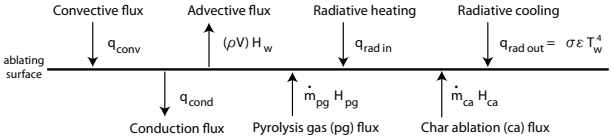

Figure 2. Energy balance at the wall

The surface energy balance at the wall depicted in figure 2 reads

$$\begin{aligned} q_{conv} - (\rho V) h_w + q_{rad,in} - q_{rad,out} - q_{cond} \\ + \dot{m}_{pg} h_{pg} + \dot{m}_{ca} h_{ca} = 0 \end{aligned} \tag{14}$$

where the convective heat flux - $q_{conv} = \rho_e u_e C'_H (h_e - h_w)$ - and the radiative heat flux are extracted from CFD simulations. The Stanton number C_H is corrected to account for the blockage induced by the pyrolysis-ablation gas-blowing; that is, the heat transfer coefficient is corrected. For example, the following correction is widely used $C'_H = C_H \, ln(1+2\lambda B')/ln(2\lambda B')$, where $B' = (\dot{m}_{pg} + \dot{m}_{ca})/(\rho_e u_e C_M)$ is a dimensionless mass flow rate and λ is a scaling factor usually taken equal to 0.5 [6].

3.2. Surface mass balance and recession rate

The pyrolysis-gas flow rate - $\dot{m}_{pg}$ - is directly obtained in the material-response code by integration of the pyrolysis, transport, and mass equations, as explained previously. However, the ablation rate - $\dot{m}_{ca}$ - is a function of both the mass transfer in the boundary layer and the thermo-chemical properties at the wall (pyrolysis-gas blowing rate and composition, temperature, pressure, boundary-layer gas composition). A common practice is to assume thermochemical equilibrium at the wall to compute the ablation rate. The model still in use in the community was developed in the sixties [27]. It is based on element conservation in steady-state in a control volume close to the wall as sketched in figure 3. The underlying hypothesis is that over a time increment Δt, the equilibrium chemistry problem in the control volume is quasi-steady (decoupling of the material response and of the boundary layer problem). This increment Δt should be at least as long as the time increment of the heat transfer simulation (material response code) but short enough so that p, T, $\dot{m}_{pg}$, and y_{pg} variations may be neglected. This is verified in typical applications. For this presentation, we shall assume equal diffusion coefficients of the elements. Failure modes (spallation, mechanical erosion) are not included and the char is assumed to be composed of a single element (for example, carbon).

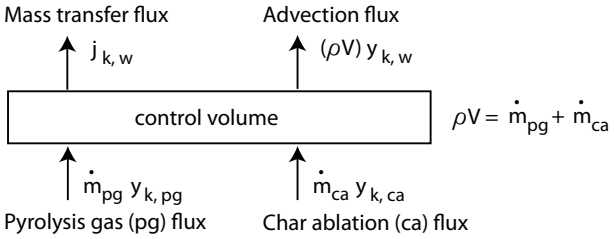

Figure 3. Element mass-fraction conservation at the wall

The inputs and outputs to this problem are:

- Inputs: $\dot{m}_{pg}$, $y_{k,pg}$, $y_{k,ca} = 1$, $y_{k,e}$, p, T.
- Outputs: $\dot{m}_{ca}$, $y_{k,w}$.

The conservation of the mass-fraction of element k in the control volume close the the wall reads:

$$j_{k,w} + (\rho V) y_{k,w} = \dot{m}_{pg} y_{k,pg} + \dot{m}_{ca} y_{k,ca} \qquad (15)$$

where pg= pyrolysis gases, ca = char ablation products, w= wall (or control volume). Notes:

- The relative mass fractions sum to 1 in each phase $\sum_k y_{k,w} = 1$; $\sum_k y_{k,pg} = 1$; $\sum_k y_{k,ca} = 1$
- Since p, T are fixed, the element mass-fraction conservation in the control volume is equivalent to the mass conservation.

Under the hypotheses that $Prandtl = Lewis = 1$ and that the diffusion coefficients are equal for the elements, equation 15 may be rewritten as

$$\rho_e u_e C_H (y_{k,w} - y_{k,e}) + (\rho V) y_{k,w} = \dot{m}_{pg} y_{k,pg} + \dot{m}_{ca} y_{k,ca} \qquad (16)$$

where, C_H is the Stanton number and $(\rho V) = \dot{m}_{pg} + \dot{m}_{ca}$.

The formation reaction of species A_i may be written:

$$A_i \rightleftharpoons \sum_{k \in Elements} \nu_{i,k} A_k \qquad (17)$$

The i chemical equilibriums read:

$$\sum_{k \in Elements} \nu_{i,k} ln(x_k) - ln(x_i) - ln(K_i) = 0 \qquad (18)$$

with $x_i = 1$ if A_i is a solid species. Species mole fractions sum to one:

$$\sum_{i \in Species} x_i = 1 \qquad (19)$$

To sum up, the set of equations solved is:

$$\rho_e u_e C_H (y_{k,w} - y_{k,e}) + (\rho V) y_{k,w} = \dot{m}_{pg} y_{k,pg} + \dot{m}_{ca} y_{k,ca} \qquad (20)$$

$$\sum_{k \in Elements} \nu_{i,k} ln(x_k) - ln(x_i) - ln(K_i) = 0 \qquad (21)$$

with $x_i = 1$ if A_i is a solid species.

$$\sum_{i \in Species} x_i = 1 \qquad (22)$$

The base model may be extended when needed to account for multicomponent mass transfer, non-equal diffusion coefficients, failure (spallation, melting), a solid phase made of more than one element (example: SiO_2), corrections to account for heterogenous finite-rate chemistry. Current development efforts aim at fully modeling the boundary layer and coupling it to material codes, with the recession directly computed in the flow solver.

The surface pressure is an input to the material code (obtained from CFD simulations). It is the boundary condition required for the averaged momentum equation.

4. SIMULATION TOOLS

More than twenty ablative-material response tools are currently in use or in development for hypersonic re-entry

applications. The name of the codes and useful information are provided in table 1. The contact listed is either the code developer or a current active user. For each code, one open-literature reference is provided (for most of them, many are however available). Our understanding of the current code capabilities and/or development strategies based on open-literature publications are summarized in figure 4.

5. CONCLUSION

A review of the governing equations and boundary conditions used to model the response of ablative materials submitted to a high-enthalpy flow has been proposed. The heritage of model-development efforts undertaken in the 1960s is extremely clear: the bases of the models used in the community are mathematically equivalent. Most of the design-rated material-response codes implement a single model in which the equation parameters may be modified to model different materials or conditions. The level of fidelity of the models implemented in design tools only slightly varies. Research and development codes developed for analysis - at least in a first stage - are generally more advanced but often not fully capable. To sum-up, more than twenty codes are currently in use or in development, with an active community both maintaining state-of-the-art capability and seeking to increase the fidelity of the state-of-the-art model.

ACKNOWLEDGMENTS

This research was partly supported by the Hypersonics Project of the NASA fundamental aeronautics program. Acknowledgments are in advance made to any contributor that will provide corrections or addenda to the (necessarily) non-exhaustive list of codes provided.

REFERENCES

[1] H.-K. Ahn, C. Park, and K. Sawada. Response of heatshield material at stagnation point of pioneer-venus probes. *Journal of Thermophysics and Heat Transfer*, 16(3):432–439, July-September 2002.

[2] G. C. April. *Energy transfer in the char zone of a charring ablator*. PhD thesis, Louisiana State University, 1969. Also, NASA CR 107533.

[3] A. R. Bahramian, M. Kokabi, M. H. N. Famili, and M. H. Beheshty. Ablation and thermal degradation behaviour of a composite based on resol type phenolic resin: Process modeling and experimental. *Ploymers*, 47:3661–3673, 2006.

[4] A. Bhatia and S. Roy. Pyrolysis gas flow in thermally ablating media using time-implicit discontinuous Galerkin methods. *AIAA paper*, 2011-145:15 p., 2011.

[5] R. Bond, D. Potter, D. Kuntz, A. Amar, and J. Smith. Aerothermal capabilities at sandia national laboratories. Technical report, Approved for unlimited release as SAND 2005-4513P, 2005.

[6] Y. K. Chen and F. S. Milos. Ablation and thermal response program for spacecraft heatshield analysis. *Journal of Spacecraft and Rockets*, 36(3):475–483, 1999.

[7] Y. K. Chen and F. S. Milos. Three-dimensional ablation and thermal response simulation system. *AIAA paper*, page 15 p., 2005. 2005-5064.

[8] D. M. Curry. An analysis of a charring ablation thermal protection system. Technical report, NASA TN D-3150, 1965.

[9] J. A. Dec and R. D. Braun. Ablative thermal response analysis using the finite element method. In *AIAA paper*, number 2009-259, 2009.

[10] H. J. Ene and E. Sanchez-Palencia. On thermal equation for flow in porous media. *International Journal of Engineering Science*, 20:623–630, 1982.

[11] M. E. Ewing and D. E. Richardson. Phenomena and material property requirements for a combined structural and thermal ablation model. In *Proc.* 4^{th} *AF/SNL/NASA Ablation Workshop*, Albuquerque, New Mexico, March 2011.

[12] V. Giovangigli. *Multicomponent flow modeling*. Birkhäuser, Boston, 1999.

[13] R. Gosse and G. Candler. Ablation modeling of electro-magnetic launched projectile for access to space. In *AIAA paper*, number 2007-1210, 2007.

[14] L. B. Hillberg. The convective heating and ablation program (chap). Technical report, Boeing Report No. D2-36402-1, 1966.

[15] A. Inc. Aerotherm charring material thermal response and ablation program - version 3. Technical report, Aerotherm report UM-70-14, 1970.

[16] R. M. Kendall, E. P. Bartlett, R. A. Rindal, and C. B. Moyer. An analysis of the coupled chemically reacting boundary layer and charring ablator: Part I. *NASA CR*, 1060, 1968. 96 p.

[17] D. W. Kuntz, B. Hassan, and D. L. PotterĞ. Predictions of ablating hypersonic vehicles using an iterative coupled fluid/thermal approach. *Journal of Thermophysics and Heat Transfer*, 15:129–139, 2001.

[18] J. Lachaud, I. Cozmuta, and N. N. Mansour. Multiscale approach to ablation modeling of phenolic impregnated carbon ablators. *Journal of Spacecraft and Rockets*, 47(6):910–921, 2010.

[19] J. Lachaud and N. N. Mansour. A pyrolysis and ablation toolbox based on openfoam - with application to material response under high-enthalpy environments. In *5th OpenFOAM Workshop*, Gothenburg, Sweden, June 2010. Chalmers University.

[20] J. Lachaud, N. N. Mansour, A. Ceballos, D. Pejakovic, L. Zhang, and J. Marschall. Validation of

Table 1. List of currently available simulation tools

Name	Contact	Owner	Users	Applications	References
Amaryllis	T. van Eekelen	Samtech, Belguim	EADS Astrium, ESA	Design	[39]
CAMAC	W.-S. Lin	CSIST, Taiwan	Taiwan Ins. of Sci. Tech.	Unknown	[21]
CAT	N. N. Mansour	NASA ARC, USA	NASA ARC	Analysis	[22]
CHALEUR	B. Blackwell	SNL, USA	SNL	Design	[5]
CHAP	P. Keller	Boeing, USA	Boeing	Design	[14]
CMA	R. Beck	Aerotherm, USA	NASA, SNL	Design	[15]
CMA/SCMA	C. Park	Tokyo Univ., Japan	JAXA	Design	[1]
CMA/KCMA	P. Reygnier	ISA, France	ISA/ESA	Analysis	[30]
COYOTTE2	D. W. Kuntz	SNL, USA	SNL	Design	[17]
FABL	J. Merrifield	Fluid Grav. Eng. Ltd., UK	ISA/ESA/FGE	Analysis	[32]
FIAT	Y.-K. Chen	NASA ARC, USA	NASA, SpaceX	Design	[6]
FIAT3D	Y.-K. Chen	NASA ARC, USA	NASA ARC	Analysis	[7]
HERO	M. E. Ewing	ATK, USA	ATK	Analysis	[11]
ITARC	M. E. Ewing	ATK, USA	ATK	Design	[11]
libAblation	R. R. Upadhyay	Univ. of Tex. Aust., USA	UTA	Analysis	[38]
MIG	S. Roy	Univ. of Flo., USA	Univ. of Florida	Analysis	[4]
MOPAR	A. Martin	Univ. of Mich., USA	UKY/Univ. of Michigan	Analysis	[24]
NEQAP	J. B. Scoggins	N. Carol. St. Univ., USA	NCSU	Analysis	[31]
NIDA	G. C. Cheng	Univ. Alab. Birm., USA	UAB	Analysis	[42]
PATO	J. Lachaud	NASA ARC, USA	Univ. Calif. Santa Cruz	Analysis	[19]
PRESENT	J. Dec	NASA LaRC, USA	NASA LaRC	Analysis	[9]
STAB	B. Remark	NASA JSC, USA	Fluid Gr. Eng.	Design	[8]
TITAN	F. S. Milos	NASA ARC, USA	NASA	Analysis	[26]
TMU	A. R. Bahramian	T. Modares Univ., Iran	TMU	Analysis	[3]
US3D	G. Candler	Univ. of Minn., USA	UM	Analysis	[13]

a volume-averaged fiber-scale model for the oxidation of a carbon-fiber preform. In A. Paper, editor, *42nd AIAA Thermophysics Conference*, number to appear, Honolulu, Hawaii, June 2011.

[21] W.-S. Lin. Quasi-steady solutions for the ablation of charring materials. *International Journal of Heat and Mass Transfer*, 50:1196Ű–1201, 2007.

[22] N. N. Mansour, J. Lachaud, T. E. Magin, J. de Muelenaere, and Y.-K. Chen. High-fidelity charring ablator thermal response model. In A. Paper, editor, *42nd AIAA Thermophysics Conference*, number to appear, Honolulu, Hawaii, June 2011.

[23] J. Marschall and F. S. Milos. Gas permeability of rigid fibrous refractory insulations. *Journal of Thermophysics and Heat Transfer*, 12:528–535, 1998.

[24] A. Martin and I. Boyd. Simulation of pyrolysis gas within a thermal protection system. In AIAA, editor, *40th Thermophysics Conference, Seattle, Washington, June 23-26*, number 3805, page 20 p., 2008.

[25] E. A. Mason and A. P. Malinauskas. *Gas transport in porous media: the dusty-gas model*. Chemical engineering monographs, Elsevier, Amsterdam, 1983.

[26] F. S. Milos and Y. K. Chen. Two-dimensional ablation, thermal response, and sizing program for pyrolyzing ablators. In *AIAA paper*, number 2008-1223, 2008.

[27] C. B. Moyer and M. R. Wool. Aerotherm equilibrium surface thermochemistry computer program - version 3. Technical report, Aerotherm, April 1970. AD875385.

[28] R. W. Pike, G. C. April, and E. G. del Valle. Nonequilibrium flow and the kinetics of chemical reactions in the char zone. *NASA status report - Grant NGR 19-001-016*, 1967. 96 p.

[29] N. Puiroux, M. Prat, and M. Quintard. Nonequilibrium theories for macroscale heat transfer: ablative composite layer system. *International Journal of Thermal Sciences*, 43:541–554, 2004.

[30] P. Reynier. Numerical rebuilding of graphite ablative test case using kcma. In *Proceedings of the Sixth European Workshop on Thermal Protection Systems and Hot Structures*, University Stuttgart, Germany, 21-25 November 2009. European Space Agency - WPP-319.

[31] J. B. Scoggins. The development of a thermochemical nonequilibrium ablation and pyrolysis model for carbon-phenolic thermal protection systems. Master's thesis, North Carolina State University, Raleigh, North Carolina, May 2011.

[32] A. J. Smith. Fabl3, a program for analysing charring ablation thermal protection systems. Technical report, Fluid Gravity Engineering TN20/96 Issue 3, 2000.

[33] M. Stackpoole, S. Sepka, I. Cozmuta, and D. Kontinos. Post-flight evaluation of stardust sample return

capsule forebody heatshield material. *AIAA paper*, 1202, January 2008. 12 p.

[34] G. F. Sykes. Decomposition characteristics of a char-forming phenolic polymer used for ablative composites. *NASA TN*, D-3810, 1967. 20 p.

[35] H. K. Tran, C. E. Johnson, D. J. Rasky, F. C. L. Hui, M.-T. Hsu, T. Chen, Y. K. Chen, D. Paragas, and L. Kobayashi. Phenolic impregnated carbon ablators (pica) as thermal protection systems for discovery missions. Technical Report 110440, NASA Technical Memorandum, 1997.

[36] K. A. Trick and T. E. Saliba. Mechanisms of the pyrolysis of phenolic resin in a carbon/phenolic composite. *Carbon*, 33(11):1509–1515, 1995.

[37] K. A. Trick, T. E. Saliba, and S. S. Sandhu. A kinetic model of the pyrolysis of phenolic resin in a carbon/phenolic composite. *Carbon*, 35(3):393–401, 1997.

[38] R. R. Upadhyay, P. Bauman, R. Stogner, K. W. Schulz, and O. A. Ezekoye. Steady-state ablation model coupling with hypersonic flow. In *AIAA paper*, number 2010-1176, 2010.

[39] T. van Eekelen, J.-M. Bouilly, S. Hudrisier, J.-M. Dupillier, and Y. Aspa. Design and numerical modelling of charring material ablators for re-entry applications. In *Proceedings of the Sixth European Workshop on Thermal Protection Systems and Hot Structures*, University Stuttgart, Germany, 21-25 November 2009. European Space Agency - WPP-319.

[40] T. van Eekelen and J. Lachaud. Radiation heat-transfer model for the ablation zone of low-density carbon-resin composites. AIAA paper 2010-4904.

[41] T. van Eekelen and J. Lachaud. Numerical validation of an effective radiation heat transfer model for fiber preforms. *Journal of Spacecraft and Rockets*, in the press, to appear 2011. Engineering note.

[42] B. S. Venkatachari, G. C. Cheng, R. P. Koomullil, and A. Ayasoufi. Computational tools for re-entry aerothermodynamics: Part II. Surface ablation. In *46th AIAA Aerospace Sciences Meeting and Exhibit*, number AIAA 2008-1218, 2008. 12 p.

Code capabilities Green : verified Yellow : under verification/to be released Red : in development	AMARYLLIS	CAMAC	CAT	CHALEUR	CHAP	CMA	CMAS	CMAK	COYOTTE2	FABL	FIAT	FIAT3D	HERO	ITRAC	LIBABLAT	MIG	MOPAR	NEQAP	NIDA	PATO	PRESENT	STAB	TITAN	TMU	US3D MOD
Summary																									
Model fidelity (1-3)	2	1	3	2	1	2	2	2	1	2	1	1	2	2	1	2	2	2	3	3	1	1	1	1	1
Code dimensionality (nD= 1-3)	3	1	1	1	1	1	1	1	3	1	1	3	3	1	1	1	1	1	1	3	1	1	2	1	1
Code maturity level (1-3)	3	1	2	2	2	3	3	3	2	2	3	2	2	3	1	1	2	1	1	2	2	3	3	2	1
Gas-phase Mass Conservation	In-depth : Eq. 1																								
Storage (∂_t ...)																									
Divergence (∂_x...)																									
Pyrolysis production (Π)																									
Pyrolysis model	In-depth: Eq. 2-7																								
SoA Arrhenius laws (-> Π)																									
Species production (-> π_i)																									
Gas-species Conservation	In-depth: Eq. 8																								
Storage (∂t ...)																									
Divergence (∂x...)																									
Multi-component diffusion ($\partial x F$)																									
Finite-rate chemistry (π_i , ω_i)																									
Solid-phase mass conservation	In-depth: Eq. 9-10																								
Pyrolyzing matrix mass loss																									
In-depth ablation/coking																									
Momentum conservation	In-depth: Eq. 11																								
Darcy's law																									
Klinkenberg/Forchheimer																									
Energy conservation	In-depth: Eq. 12-13																								
Storage (∂t ...)																									
Divergence (∂x...)																									
Effective conduction																									
Viscous dissipation																									
Boundary conditions	At the wall: Eq. 14-22																								
Surface energy balance																									
Wall chemistry from B' table																									
Internal wall chemistry solver																									
Other utilities	Integrated libraries																								
Equilibrium chemistry solver																									
Integrated boundary layer code																									
Script -coupling to CFD code																									

Figure 4. Simulation-tool list and capabilities. [The authors wish to apology in advance for any missing or incorrect information contained in this figure. Corrections and addenda will be greatly appreciated.]

A short review of ablative-material response models & simulation tools

Jean Lachaud*, Thierry E. Magin', Ioana Cozmuta[x], and Nagi N. Mansour[+]

*Univ. of California Santa Cruz/UARC, Jean.Lachaud@nasa.gov
' von Karman Institute, magin@vki.ac.be
[x] ERC, Ioana.Cozmuta@nasa.gov
[+] NASA Ames Research Center, Nagi.N.Mansour@nasa.gov
***Sponsored by NASA's Fundamental Aeronautics Program - Hypersonics Project**

7th Aerothermodynamics Symposium (European Space Agency)
9 - 12 May 2011, Site Oud Sint-Jan, Brugge, Belgium

Session : Thermal Protection Systems

ablation

. Introduction

Physics and Chemistry in Ablative Materials

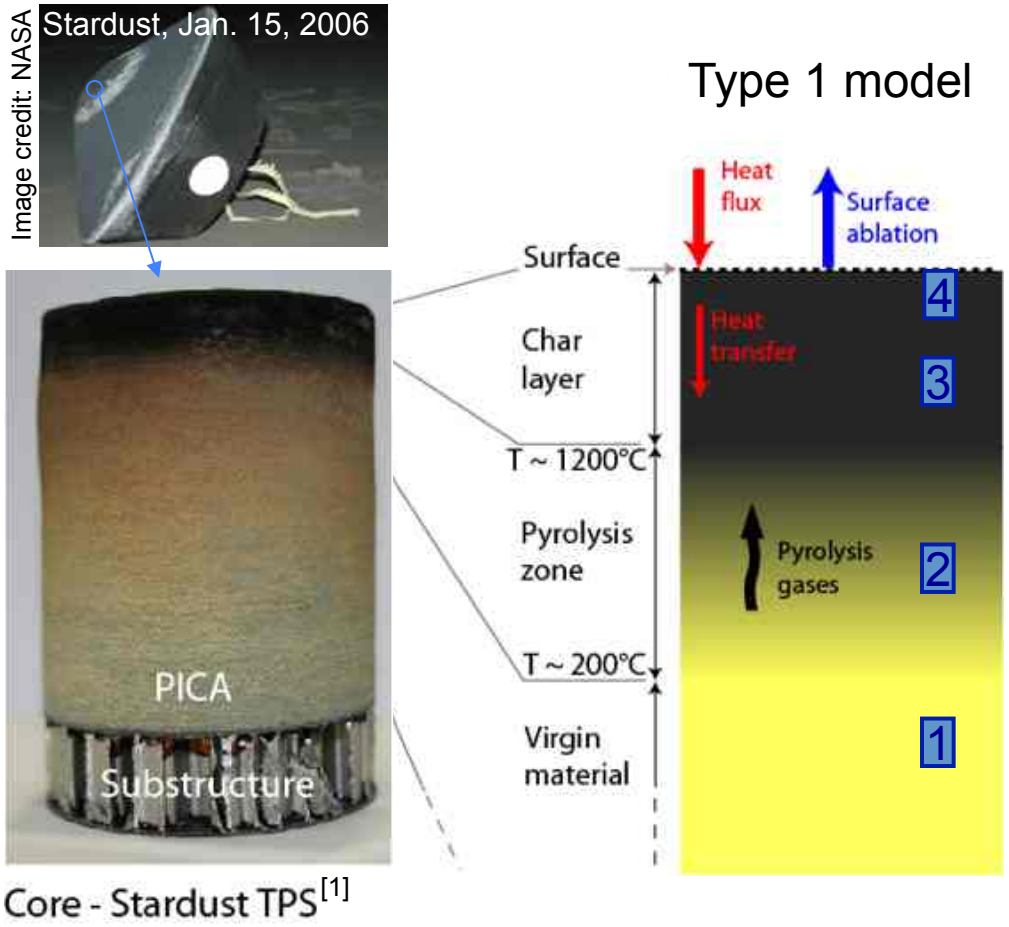

Core - Stardust TPS[1]

Color code for the presentation

Three types of material-response models have been identified & defined [during the **4th AFOSR/ SNL/NASA Ablation Workshop. March 1-3, 2011, Albuquerque, NM**]:

- **Type 1**: Heat transfer, pyrolysis, simplified transport of the pyrolysis gases, equilibrium chemistry, surface ablation (current state-of-the-art)
- **Type 2**: **Type 1** + averaged momentum equation for the transport of the pyrolysis gases (e.g. Darcy's law)
- **Type 3**: **High-fidelity model** (**Type 2** + finite-rate chemistry, multi-component diffusion, in-depth ablation/coking, explicit radiative transfer model, …)

SEM micrographs [1]

[1] M. Stackpoole *et al.,* Post-Flight Evaluation of Stardust Sample Return Capsule Forebody Heatshield Material, AIAA 2008-1202

. Outline

Motivation: Pure curiosity, review currently available codes and models

1 – In-depth modeling

- **1.1 – Mass conservation**
- **1.2 – Mass transport**
- **1.3 – Energy conservation**

2 – Boundary conditions

- **2.1 – Surface energy balance**
- **2.2 – Surface mass balance and recession rate**

3 – Summary

- **3.1 – Table 1: List of codes, contacts, and references**
- **3.2 – Table 2: Codes capabilities**

1.1. Mass conservation (gas/solid system)

Candid illustration of the chemistry of Pyrolysis & Ablation : incomplete mechanism!

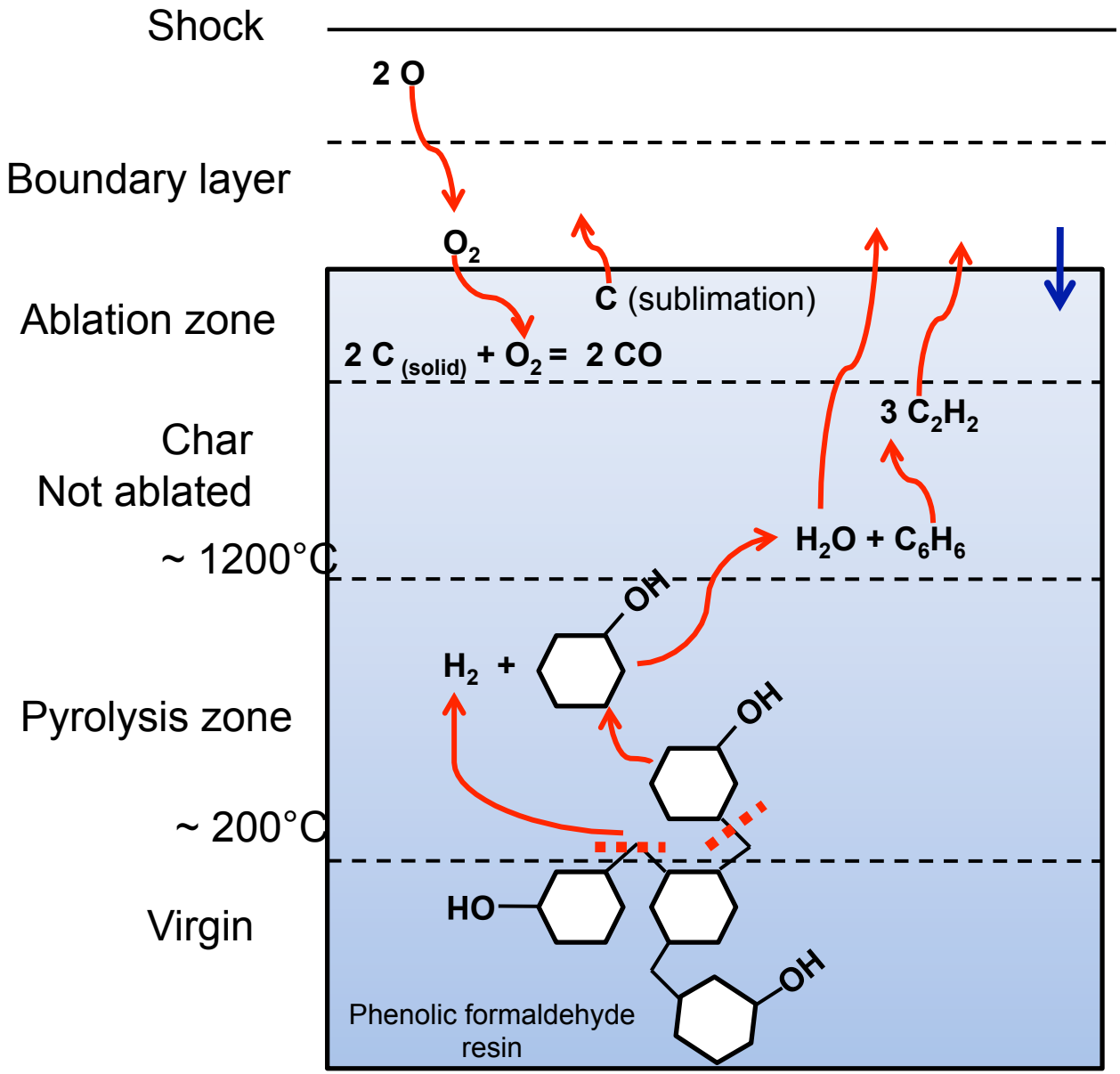

Ablation (leads to surface recession)

Chemistry of the pyrolysis gases

Pyrolysis & Pyrolysis-gas production

1.1. Mass conservation (gas/solid system)

Models: Type 1 / Type 2 / Type 3 - In green: Experiments -

Type 1 codes - hypothesis: instantaneous transfer (no storage)

$$\partial_x \cdot \left(\dot{m}_g \right) = \Pi$$

Pyrolysis gas flux

Pyrolysis laws (Arrhenius) = f(Temperature)
- Thermogravimetry analysis (TGA)

Type 2 & Type 3

$$\partial_t \left(\varepsilon_g \rho_g \right) + \partial_x \cdot \left(\varepsilon_g \rho_g \vec{v}_g \right) = \Pi$$

Open porosity
- Pycnometry

$$\rho_g = \frac{pM}{RT}$$

see Momentum Conservation

Mean molar mass: $M = \sum_i x_i M_i$

Need to determine Gas Composition (in mole fractions of the species)

Equilibrium chemistry + elemental composition

Finite-rate chemistry + species conservation

1.1. Species conservation (gas/solid system)

Models: Type 1 / Type 2 / Type 3 - In green: Experiments -

• **Gaseous Species Conservation**

$$\partial_t\left(\varepsilon_g \rho_g y_i\right) + \partial_x \cdot \left(\varepsilon_g \rho_g y_i \vec{v}_i\right) = \pi_i M_i + \varepsilon_g \omega_i M_i$$

- $\partial_t\left(\varepsilon_g \rho_g y_i\right)$: Mass fraction of species i
- $\vec{v}_i$: See mass transport
- $\pi_i M_i$: Pyrolysis production rate for each species
  -Thermogravimetry analysis (TGA) + mass spectroscopy / chromatography
- $\varepsilon_g \omega_i M_i$: Finite-rate chemistry mechanism
  - Flow reactor + spectro/chromato

• **Solid-phase volume-fraction conservation** (in-depth ablation/ coking)

Porosity increase/decrease due to heterogeneous reactions

– hypotheses: no swelling, constant intrinsic solid densities --

Fibers : $\partial_t \varepsilon_f = -\Omega_f \sum_{i \in S} \varepsilon \omega_i$ Carbonized matrix : $\partial_t \varepsilon_m = -\Omega_m \sum_{i \in S} \varepsilon \omega_i$

Ω: Molar volume

Quantification of porosity change/heterogeneous chemistry
-Scanning Electron Spectroscopy (SEM) / Tomography before and after testing.

1.1. Species conservation (gas/solid system)

Pyrolysis-gas SPECIES-production modeling

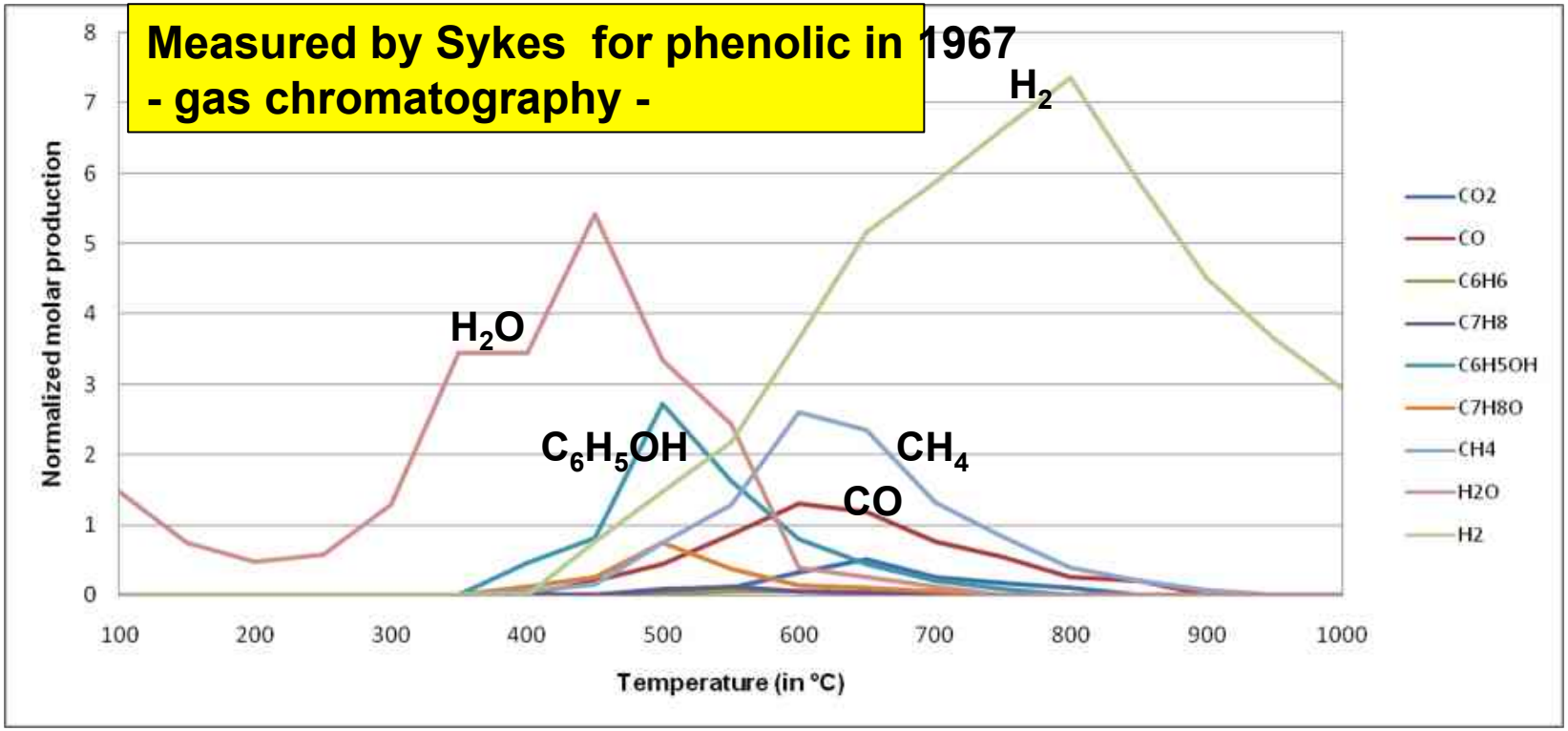

j	Pyrolysis balance equations	Peak	F_j	$\mathcal{A}_j$	$\mathcal{E}_j$	m_j	n_j
	Inferred from Sykes 1967 [19]	[19, 21]	[19]	Trick [21]	[21]	[21]	[21]
1	$PFR_1 \rightarrow H_2O\,(physisorbed)$	$100°C$	(0.02)*	-	-	-	-
2	$PFR_2 \rightarrow 0.69\,H_2O + 0.01C_6H_6$ $+0.01C_7H_8 + 0.23\,C_6H_6O + 0.06\,C_7H_8O$	$500°C$	0.73	$1.9 \cdot 10^3$	$9.8 \cdot 10^4$	1	1
3	$PFR_3 \rightarrow 0.09\,CO_2 + 0.33\,CO + 0.58\,CH_4$	$600°C$	0.21	11	$7.7 \cdot 10^4$	1	1
4	$PFR_4 \rightarrow H_2$	$800°C$	0.06	$6.6 \cdot 10^6$	$2.0 \cdot 10^5$	1	1

1.1. Species conservation (gas/solid system)

Finite-rate chemistry of the pyrolysis gases

Table 6-6. Important Reactions and Associated Kinetic Data for the Pyrolysis Product Species in the Char Zone Between 500-3000°F.

General Form of the Reactions: $aA + bB + \ldots + = rR + sS + \ldots +$

General Rate Constant Equation: $k = k^{\circ}T^{-s}\,\mathrm{Exp}(-E/RT)$

Reaction Number	Reaction	Rate Law	Activation Energy E, Kcal/gm-mole)	Frequency Factor	s	References
(6-1)	$CH_4 = 1/2\ H_2 + 1/2\ C_2H_6$	k_fA	95.0	7.6×10^{14} *	0	14,15,16,17 18,19
(6-2)	$C_2H_6 = C_2H_4 +$					14,20,16,17 18,21
(6-3)	$C_2H_4 = C_2H_2 +$					14, 16
(6-4)	$C_2H_2 = 2C + H_2$	k_fA^2	10.0	2.1×10^{10} **	0	14,22,28
(6-5)	$C + 2H_2 = CH_4$	k_f	17.0	2.0×10^{9} ***	0	30,31,23,24 25,26,32
(6-6)	$C_6H_6O + H_2 = H_2O + C_6H_6$	k_fA	45.0	2.0×10^{13} *	0	49
(6-7)	$C_6H_6 = 3\ C_2H_2$	k_fA	35.0	1.4×10^{9} *	0	33
(6-8)	$C + H_2O = CO + H_2$	k_fAB	82.0	1.2×10^{12} **	-1	42,47,35,36 38,39,40,43
(6-9)	$CO + H_2O = H_2 + CO_2$	k_fAB	30.0	1.0×10^{12} **	0	41,35,36,38 39,40,43,44
(6-10)	$C + CO_2 = 2\ CO$	$k_fA-k_rR^2$	50.0 61.0	1.0×10^{6} * 1.0×10^{-9} **	-1 0	45,46,35,36 38,39,40,44

* 1st Order (sec^{-1}) ** 2nd Order (cm^3/gm-mole-sec) *** 0th Order (gm-mole/cm^3-sec)

$C_6H_6O + H_2 = H_2O + C_6H_6$

[April69] April, G. C., "Energy Transfer in the char Zone of a Charring Ablator", Ph. D. Dissertation, Department of Chemical engineering, Louisiana State University, 1969.

1.1. Mass conservation (gas/solid system)

Illustration: oxidation of a carbon preform.

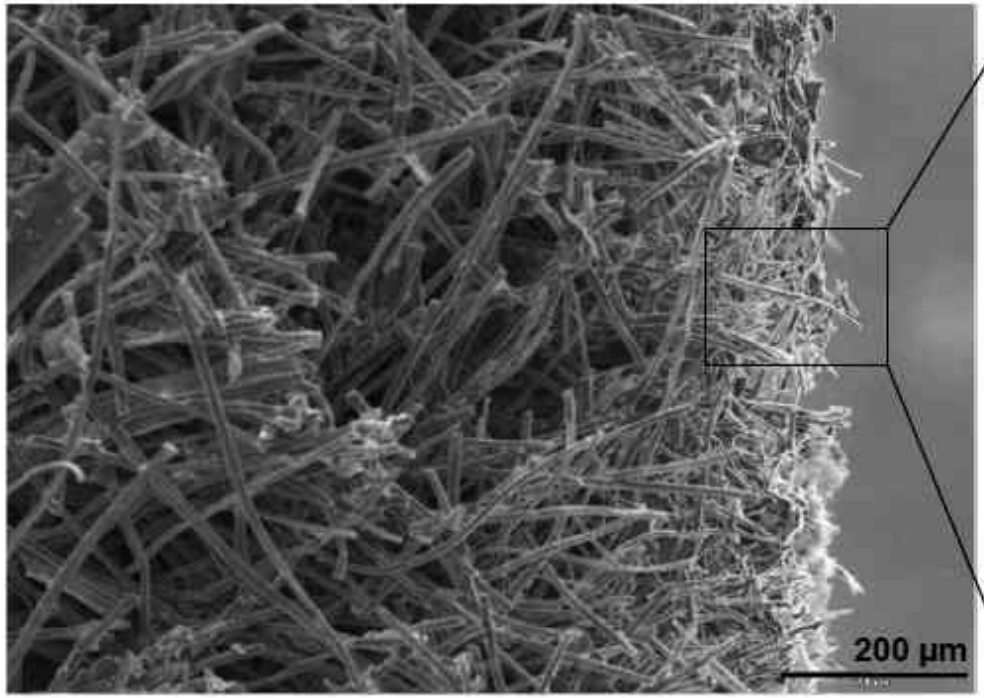

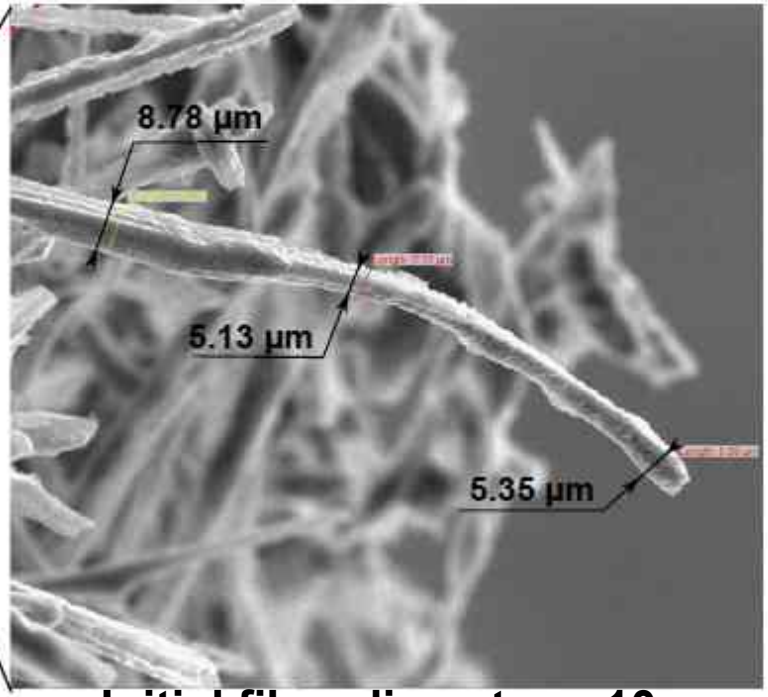

Initial fiber diameter ≈ 10 µm

p = 0.12 atm ; T=898 K -> Recession: 0.7 cm in 1 hour.

Two principal observations:

- reduction of fiber diameter eventually leading to recession
- sharp ablation front (about 0.2 mm) [i.e. oxygen is quickly consumed, reaction >> transpor

Validation of a volume-averaged fiber-scale model for the oxidation of a carbon-fiber preform.
J Lachaud, N N Mansour, Joe Marschall, et al. To appear, 42nd AIAA Thermophysics Conference, 27-30 June 2011.

1.2. Mass transport in porous media

Models: Type 1 / Type 2 / Type 3 - In green: Experiments -

Species velocity → $\mathbf{v}_i = \mathbf{v}_g + \mathbf{V}_i$

Average gas velocity

Diffusion velocity

Momentum Conservation in porous media

$$\mathbf{v}_g = -\frac{1}{\varepsilon_g}\frac{K}{\mu}\frac{1+\beta/p}{1+Fo}\partial_x p$$

Generalization of Darcy's law

K: permeability
β: Klinkenberg coefficient (low density,
slip effect) –typically p < 0.1 atm
Fo: Forchheimer number (high velocity,
separation) – typically v_g > 50 m/s
- Permeameter
- Tomography + DNS

μ: viscosity, computed from the gas composition, cf options for M

Multicomponent mass transfer in porous media

(e.g. Dusty Gas Model: Stefan-Maxwell + Bosanquet)

In porous media, the effective diffusion coefficient is reduced (because wall collisions decrease the effective mean free path)

$$D_{eff} = \frac{\varepsilon_g}{\eta} D_{ref}$$

Tortuosity
- Diffusivity apparatus
- Tomography + DNS

1.3. Energy conservation

Models: Type 1 / Type 2 / Type 3 - In green: Experiments -

Thermal equilibrium between the phases studied by N. Puiroux [AIAA 2002-3336]. His conclusion is that the thermal equilibrium assumption is valid.

One temperature model

$$\partial_t(\rho_a e_a) + \partial_x.(\varepsilon_g \rho_g h_g \vec{v}_g) = \partial_x \cdot (\underline{\underline{k}} \cdot \partial_x T) + \partial_x \sum_{i \in S} \varepsilon_g \rho_g y_i h_i \vec{V}_i + \mu \varepsilon^2 \underline{\underline{K}}^{-1} \cdot v \cdot v$$

computed

computed

computed

$$\rho_a e_a = \varepsilon_g \rho_g e_g + \varepsilon_m \rho_m h_m + \varepsilon_f \rho_f h_f$$

Computed or neglected

Solid enthalpies
-Differential Scanning Calorimetry (DSC)

Effective conductivity
(conduction + radiative transfer)
- Guarded Hot Plate
- Flash diffusivity
- Arc Jet calibration

. Outline

Motivation: Pure curiosity, review currently available codes and models

1 – In-depth modeling

- **1.1 – Mass conservation**
- **1.2 – Mass transport**
- **1.3 – Energy conservation**

2 – Boundary conditions

- **2.1 – Surface energy balance**
- **2.2 – Surface mass balance and recession rate**

3 – Summary

- **3.1 – Table 1: List of codes, contacts, and references**
- **3.2 – Table 2: Codes capabilities**

2.1. Surface Energy Balance

At the wall

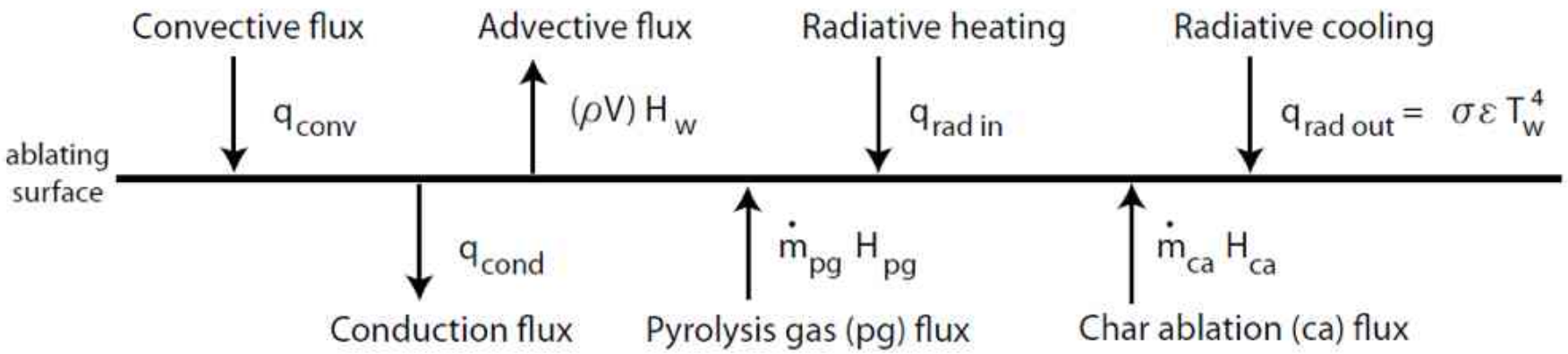

$$q_{conv} - (\rho V)h_w + q_{rad,in} - q_{rad,out} - q_{cond} + \dot{m}_{pg}h_{pg} + \dot{m}_{ca}h_{ca} = 0$$

From CFD

Unknown: mass loss rate (kg/m²/s)
-> Will provide the recession rate
$\mathbf{v_{ablation} = \dot{m}_{ca} / \rho_{char}}$

2.2. Surface mass balance and recession rate

At the wall (simplified description: equilibrium chemistry, no spallation)

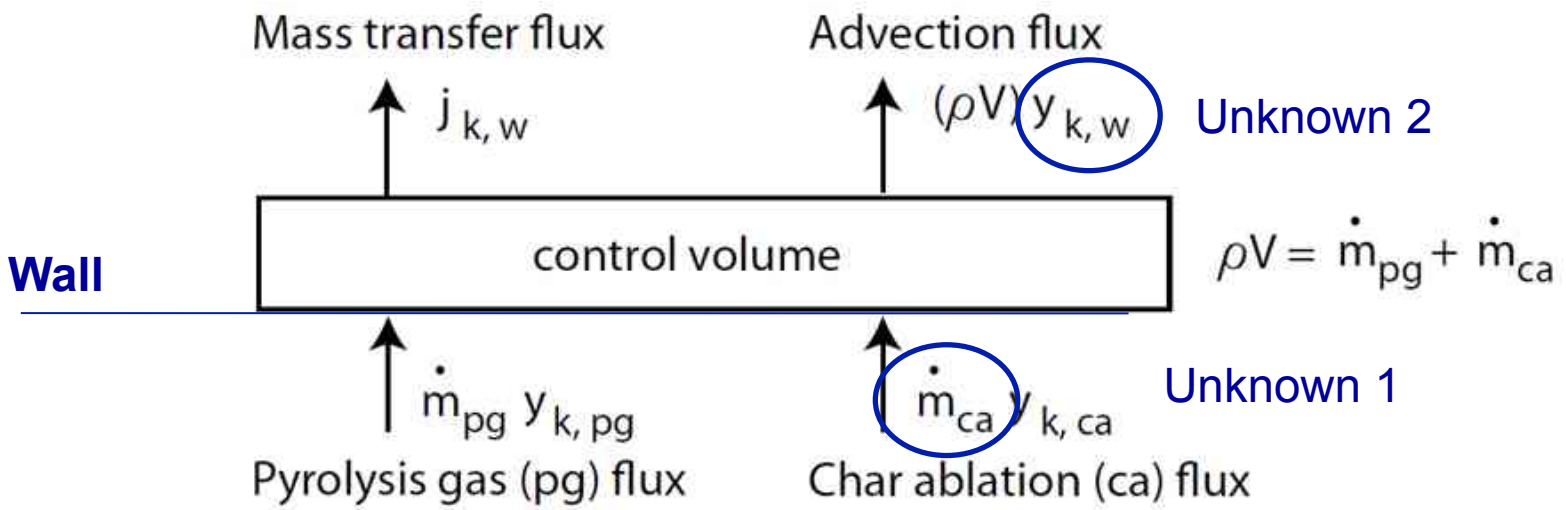

1- Conservation of element mass fraction in the control volume ($y_{k,w}$)

$$j_{k,w} + (\rho V) y_{k,w} = \dot{m}_{pg} y_{k,pg} + \dot{m}_{ca} y_{k,ca}$$

2- Equilibrium chemistry

Provides both the ablation rate $\dot{m}$ (**m_{ca}**) and the gas composition (**$y_{k,w}$**) in the control volume (and derived quantities, like **wall enthalpy**)

The dimensionless tabulation of **$\dot{m}_{ca}$ = f($\dot{m}_{pg}$, T, p)** is called a **B' table**

. Outline

Motivation: Pure curiosity, review currently available codes and models

1 – In-depth modeling

- **1.1 – Mass conservation**
- **1.2 – Mass transport**
- **1.3 – Energy conservation**

2 – Boundary conditions

- **2.1 – Surface energy balance**
- **2.2 – Surface mass balance and recession rate**

3 – Summary

- **3.1 – Table 1: List of codes, contacts, and references**
- **3.2 – Table 2: Codes capabilities**

3.1. Table 1: List of codes, contacts, and references

We found 25 codes actively used and with open-literature references…

Name	Contact	Owner	Users	Applications	References
Amaryllis	T. van Eekelen	Samtech, Belguim	EADS Astrium, ESA	Design	[17]
CAMAC	W.-S. Lin	CSIST, Taiwan	Taiwan Ins. of Sci. Tech.	Unknown	[18]
CAT	N. N. Mansour	NASA ARC, USA	NASA ARC	Analysis	[19]
CHALEUR	B. Blackwell	SNL, USA	SNL	Design	[20]
CHAP	P. Keller	Boeing, USA	Boeing	Design	[21]
CMA	R. Beck	Aerotherm, USA	NASA, SNL	Design	[22]
CMA/SCMA	C. Park	Tokyo Univ., Japan	JAXA	Design	[23]
CMA/KCMA	P. Reygnier	ISA, France	ISA/ESA	Analysis	[24]
COYOTTE2	D. W. Kuntz	SNL, USA	SNL	Design	[25]
FABL	J. Merrifield	Fluid Grav. Eng. Ltd., UK	ISA/ESA/FGE	Analysis	[26]
FIAT	Y.-K. Chen	NASA ARC, USA	NASA, SpaceX	Design	[27]
FIAT3D	Y.-K. Chen	NASA ARC, USA	NASA ARC	Analysis	[28]
HERO	M. E. Ewing	ATK, USA	ATK	Analysis	[29]
ITARC	M. E. Ewing	ATK, USA	ATK	Design	[29]
libAblation	R. R. Upadhyay	Univ. of Tex. Aust., USA	UTA	Analysis	[30]
MIG	S. Roy	Univ. of Flo., USA	Univ. of Florida	Analysis	[31]
MOPAR	A. Martin	Univ. of Mich., USA	UKY/Univ. of Michigan	Analysis	[32]
NEQAP	J. B. Scoggins	N. Carol. St. Univ., USA	NCSU	Analysis	[33]
NIDA	G. C. Cheng	Univ. Alab. Birm., USA	UAB	Analysis	[34]
PATO	J. Lachaud	NASA ARC, USA	Univ. Calif. Santa Cruz	Analysis	[35]
PRESENT	J. Dec	NASA LaRC, USA	NASA LaRC	Analysis	[36]
STAB	J. Merrifield	NASA JSC, USA	Fluid Gr. Eng.	Design	[37]
TITAN	F. S. Milos	NASA ARC, USA	NASA	Analysis	[38]
TMU	A. R. Bahramian	T. Modares Univ., Iran	TMU	Analysis	[39]
US3D	G. Candler	Univ. of Minn., USA	UM	Analysis	[40]

… please help us extending the list!

Code capabilities Green : verified Yellow : under verification/to be released Red : in development	AMARYLLIS	CAMAC	CAT	CHALEUR	CHAP	CMA	CMAS	CMAK	COYOTTE2	FABL	FIAT	FIAT3D	HERO	ITRAC	LIBABLAT	MIG	MOPAR	NEQAP	NIDA	PATO	PRESENT	STAB	TITAN	TMU	US3D MOD
Summary																									
Model fidelity (1-3)	2	1	3	2	1	2	2	2	1	2	1	1	2	2	1	2	2	2	3	3	1	1	1	1	1
Code dimensionality (nD= 1-3)	3	1	1	1	1	1	1	1	3	1	1	3	3	1	1	1	1	1	1	3	1	1	2	1	1
Code maturity level (1-3)	3	1	2	2	2	3	3	3	2	2	3	2	2	3	1	1	2	1	1	2	2	3	3	2	1
Gas-phase Mass Conservation	In-depth : Eq. 1																								
Storage (∂_t ...)																									
Divergence (∂_x...)																									
Pyrolysis production (Π)																									
Pyrolysis model	In-depth: Eq. 2-7																								
SoA Arrhenius laws (-> Π)																									
Species production (-> πi)																									
Gas-species Conservation	In-depth: Eq. 8																								
Storage (∂t ...)																									
Divergence (∂x...)																									
Multi-component diffusion ($\partial x F$)																									
Finite-rate chemistry (πi , ω_i)																									
Solid-phase mass conservation	In-depth: Eq. 9-10																								
Pyrolyzing matrix mass loss																									
In-depth ablation/coking																									
Momentum conservation	In-depth: Eq. 11																								
Darcy's law																									
Klinkenberg/Forchheimer																									
Energy conservation	In-depth: Eq. 12-13																								
Storage (∂t ...)																									
Divergence (∂x...)																									
Effective conduction																									
Viscous dissipation																									
Boundary conditions	At the wall: Eq. 14-22																								
Surface energy balance																									
Wall chemistry from B' table																									
Internal wall chemistry solver																									
Other utilities	Integrated libraries																								
Equilibrium chemistry solver																									
Integrated boundary layer code																									
Script -coupling to CFD code																									

Table 2:
Codes capabilities

Please accept our apologies for any error.
Corrections and suggestions of improvement will be greatly appreciated!

Conclusion

- **25+ codes** actively used
- **same base model** (from the 1960s)
- design-rated tools: simple and robust
- analysis and research tools: generally more advanced but often not fully capable for design
- **very active and diverse community**

APPENDICES

1.3. Energy conservation

Radiative heat transfer in fibrous preforms. 2D DNS & volume averaging

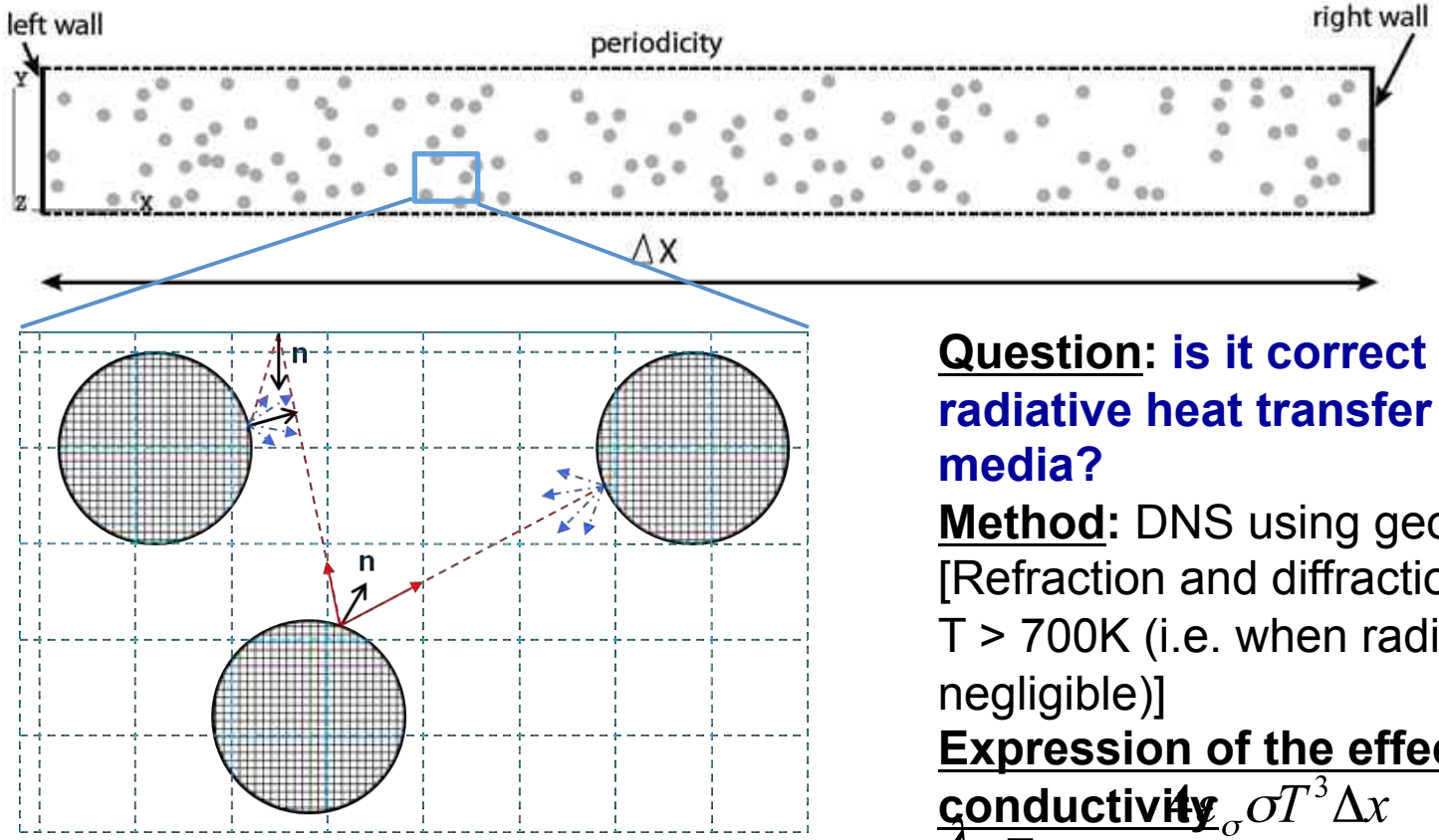

- Collision based ray-tracing algorithm to compute the form factors
- Finite-element code SAMCEF

Question: is it correct to linearize the radiative heat transfer in fibrous media?

Method: DNS using geometrical optics [Refraction and diffraction negligible for T > 700K (i.e. when radiation not negligible)]

Expression of the effective conductivity:

$$\lambda_r = \frac{4\varepsilon_\sigma \sigma T^3 \Delta x}{(2-\varepsilon_\sigma)+\sigma_{ext}\varepsilon_\sigma \rho_0 \Delta x}$$

(following linearization of the radiative transport)

Objective: compute the extinction coefficient and verify the accuracy of the effective model.

Numerical Validation of an Effective Radiation Heat Transfer Model for Fiber Preforms. T. van Eekelen, J. Lachaud. Journal of Spacecraft and Rockets. Technical note. Accepted for publication.

2.3. Sensitivity analysis

2011 ablation-modeling test-case (4th AFOSR/NASA/SNL Ablation workshop, March 1-3, 2011)

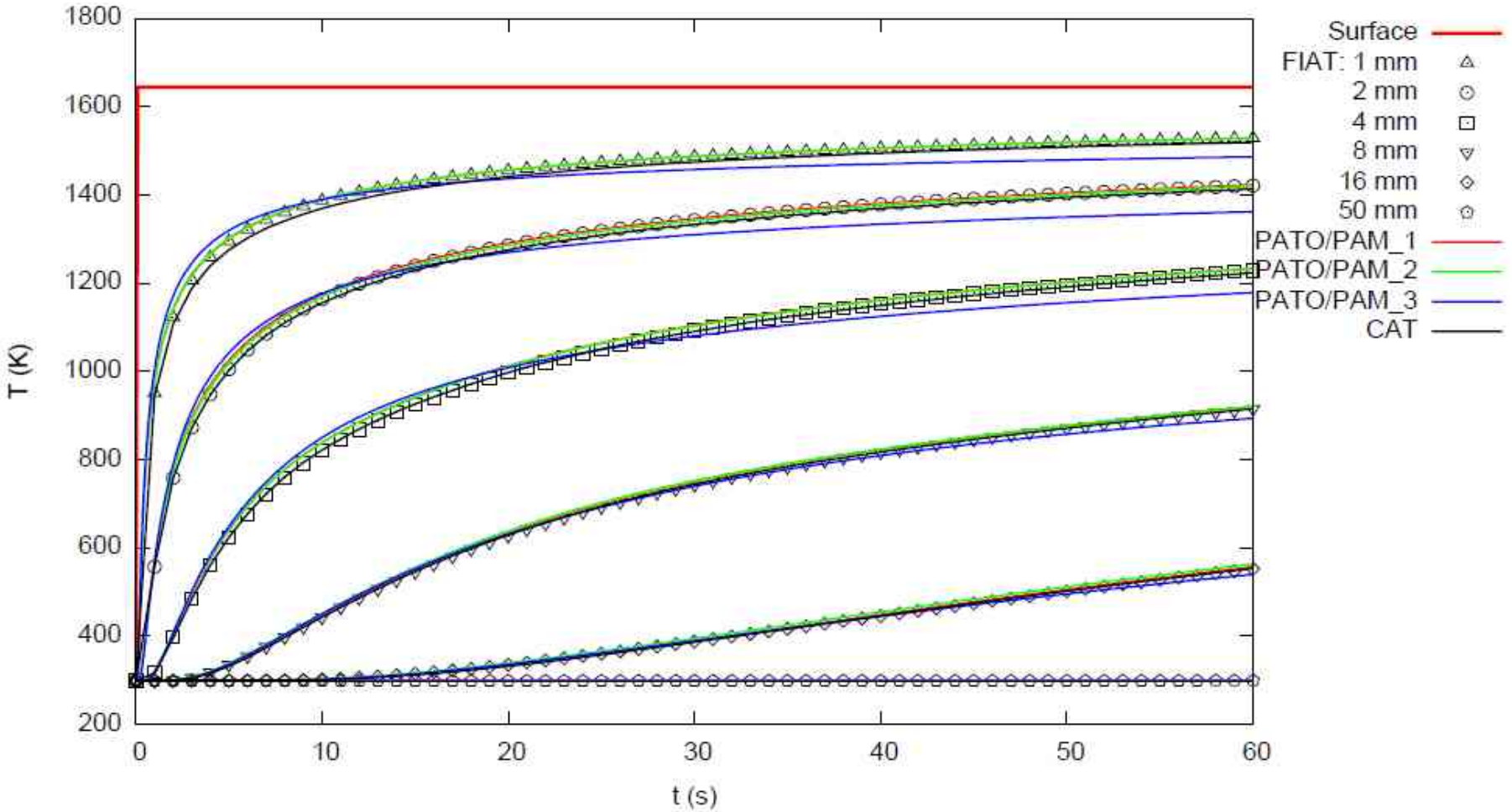

<u>14 participants</u> : we are still working on the analysis of the results, but a few remarks

- **13 codes (type 1 and/or type 2)** gave **results in agreement** with FIAT (cf. PAM_1, PAM_2, CAT). Some differences attributed to: numerical errors (+/- 1%) and misinterpretation of the data for 2 codes (+/-6%).
- **1 code out-of-range** (difference > 200%)
- **Type 3** (with finite-rate chemistry) **<u>predicts lower temperatures</u>** (PAM_3).

2.3. Sensitivity analysis

2011 ablation-modeling test-case (4th AFOSR/NASA/SNL Ablation workshop, March 1-3, 2011)

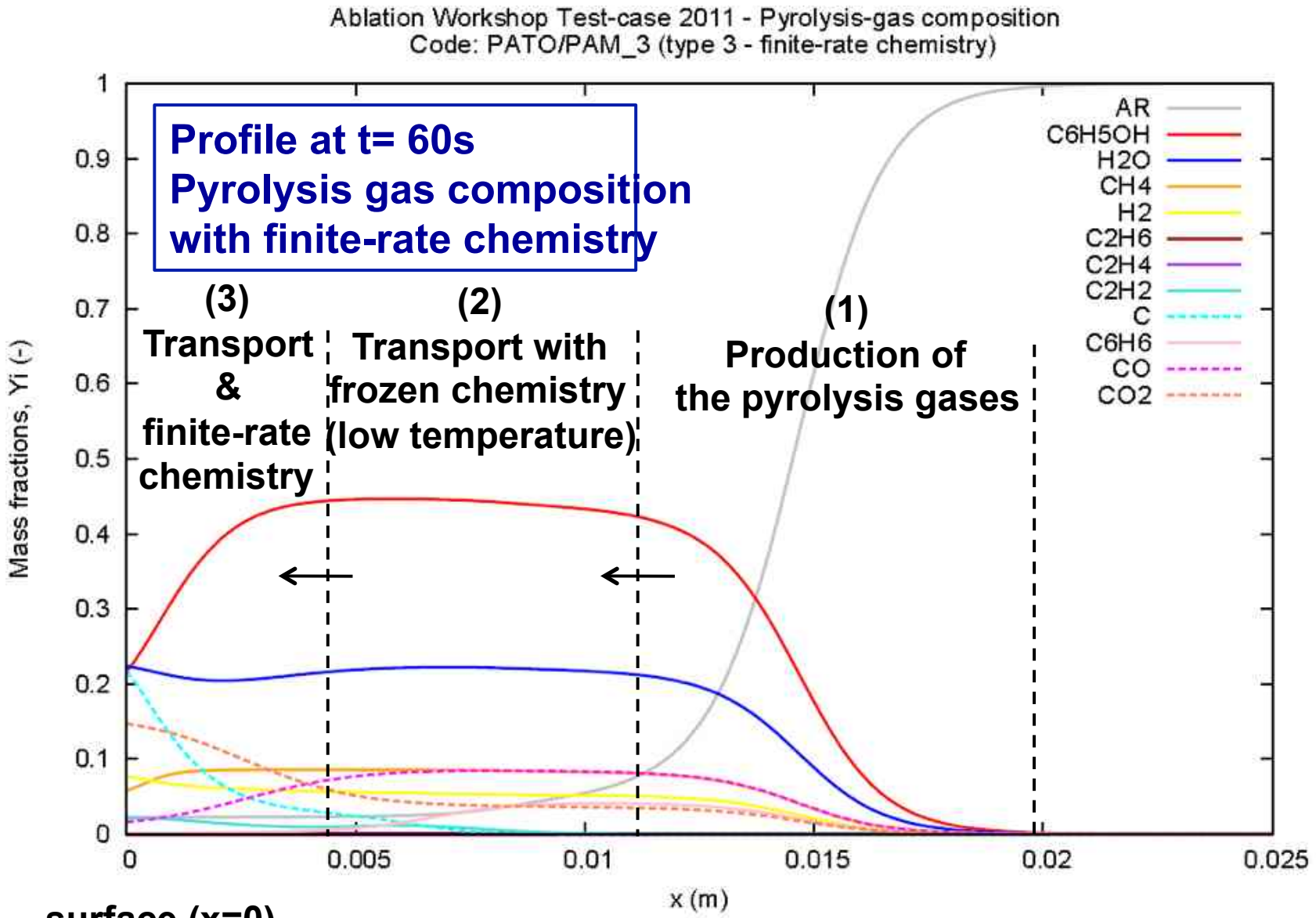

surface (x=0)